

# AEgIS Experiment at CERN: Design and Commissioning of SARA (Scintillator Assemblies to Reveal Annihilations)

**P. Conte<sup>a,b,1</sup> G. Consolati<sup>a,b</sup> M. Prata<sup>c</sup> M. Berghold<sup>d</sup> R. Caravita<sup>e</sup> R. Ferguson<sup>e,f</sup>  
M. Grosbart<sup>g</sup> F. Guatieri<sup>d,e,f</sup> S. Haider<sup>g</sup> G. Khatri<sup>g</sup> L. Lappo<sup>h</sup> P. Moskal<sup>i,j</sup> M. Münster<sup>d</sup>  
L. Penasa<sup>e,f</sup> S. Sharma<sup>i,j</sup>**

<sup>a</sup>*INFN Milano,*

*via Celoria 16, 20133 Milano, Italy*

<sup>b</sup>*Department of Aerospace Science and Technology, Politecnico di Milano,  
via La Masa 34, 20156 Milano, Italy*

<sup>c</sup>*INFN Pavia,*

*via Bassi 6, 27100 Pavia, Italy*

<sup>d</sup>*Heinz Maier Leibnitz Zentrum (MLZ), Technical University of Munich,  
Lichtenbergstraße 1, 85748, Garching, Germany*

<sup>e</sup>*TIFPA/INFN Trento,*

*via Sommarive 14, 38123 Povo, Trento, Italy*

<sup>f</sup>*Department of Physics, University of Trento,  
via Sommarive 14, 38123 Povo, Trento, Italy*

<sup>g</sup>*Physics Department, CERN,  
1211 Geneva 23, Switzerland*

<sup>h</sup>*Warsaw University of Technology, Faculty of Physics,  
ul. Koszykowa 75, 00-662, Warsaw, Poland*

<sup>i</sup>*Marian Smoluchowski Institute of Physics, Jagiellonian University,  
ul. Łojasiewicza 11, 30-348 Kraków, Poland*

<sup>j</sup>*Centre for Theranostics, Jagiellonian University,  
ul. Kopernika 40, 31-501 Kraków, Poland*

*E-mail: [pietro.conte@mi.infn.it](mailto:pietro.conte@mi.infn.it)*

**ABSTRACT:** SARA is the system of plastic scintillators coupled with silicon photomultipliers that will take part in the AEgIS experiment at CERN, measuring the time-of-flight of antihydrogen as it falls through a moiré deflectometer. Its development focused on simplicity, versatility and economy of the design and was supported by both physical tests and finite elements numerical simulations. The instrument's structure pairs the utilization of the scintillators as structural components with custom made 3D printed corner elements and the electronics allows to select between coincidence discrimination made on each scintillator and made between different scintillators.

**KEYWORDS:** Beam-line instrumentation; Photon detectors for UV, visible and IR photons (solid-state); Scintillators and scintillating fibres and light guides; Detector design and construction technologies and materials

---

<sup>1</sup>Corresponding author.

---

## Contents

<b>1</b>	<b>Introduction</b>	<b>1</b>
<b>2</b>	<b>Objective Statement, Requirements, Design and Commissioning</b>	<b>2</b>
2.1	The Objective Statement	2
2.2	SARA Major Requirements	3
2.3	Initial Design Assumptions	3
2.4	The SARA's Structure	5
2.5	The FEM Mechanical Simulations	7
2.6	The Readout Electronics	8
2.7	The SARA performance optimization	10
2.8	The SARA Commissioning	11
<b>3</b>	<b>Discussion</b>	<b>15</b>
<b>4</b>	<b>Acknowledgments</b>	<b>15</b>

---

## 1 Introduction

The AEgIS experiment (Antihydrogen Experiment: gravity, Interferometry, Spectroscopy) at CERN aims to measure the effects of Earth's gravity on antimatter in the absence of magnetic field influences and with an accuracy of 1% [1]. The results will pave the way for testing the Weak Equivalence Principle of General Relativity and the Charge, Parity and Time reversal Symmetry embedded in Quantum Field Theory [2].

The experiment will use a horizontally-boosted, free-falling pulsed beam of antihydrogen that will be sent in a moiré deflectometer, a horizontal tube kept at ultra high vacuum conditions where two horizontal gratings, placed at the beginning and in the middle, will generate a spatial periodic distribution of antihydrogen at a fixed distance from the second grid (Figures 1 (a) and (b)).

This fringe pattern will be collected by OPHANIM, a high-resolution position-sensitive 3840-Megapixel CMOS detector [4] capable of comparing the antihydrogen fringe pattern with the one of a reference light source that traveled the same path and has not been affected by gravity.

The vertical position difference measured by the detector will be introduced in the equation  $\Delta y = -\bar{g}\Delta t^2$ , giving as result the intensity of the gravity acceleration acting on antimatter. The antihydrogen transit time will be measured as the difference between the time instant at which it will arrive at OPHANIM and the one at which it will be formed, known with an uncertainty of 250 ns [5]. Antihydrogen will be obtained by forcing the interaction between antiprotons, coming from the Antimatter Decelerator (AD), and excited positronium in Rydberg states ( $Ps^*$ ), generated by shooting two laser beams (205.045 nm and 1693 nm) toward a cloud of ortho-positronium. The latter will be formed through the interaction between a positron beam, coming from a  $^{22}Na$  source,

and a porous target [6]. This antihydrogen production is called charge-exchange process and is summarized by the equation [7]:

$$Ps^* + \bar{p} \rightarrow \bar{H}^* + e^- \quad (1.1)$$

The Gravity Module of the AEgIS apparatus is shown in Figures 1 (c) and (d).

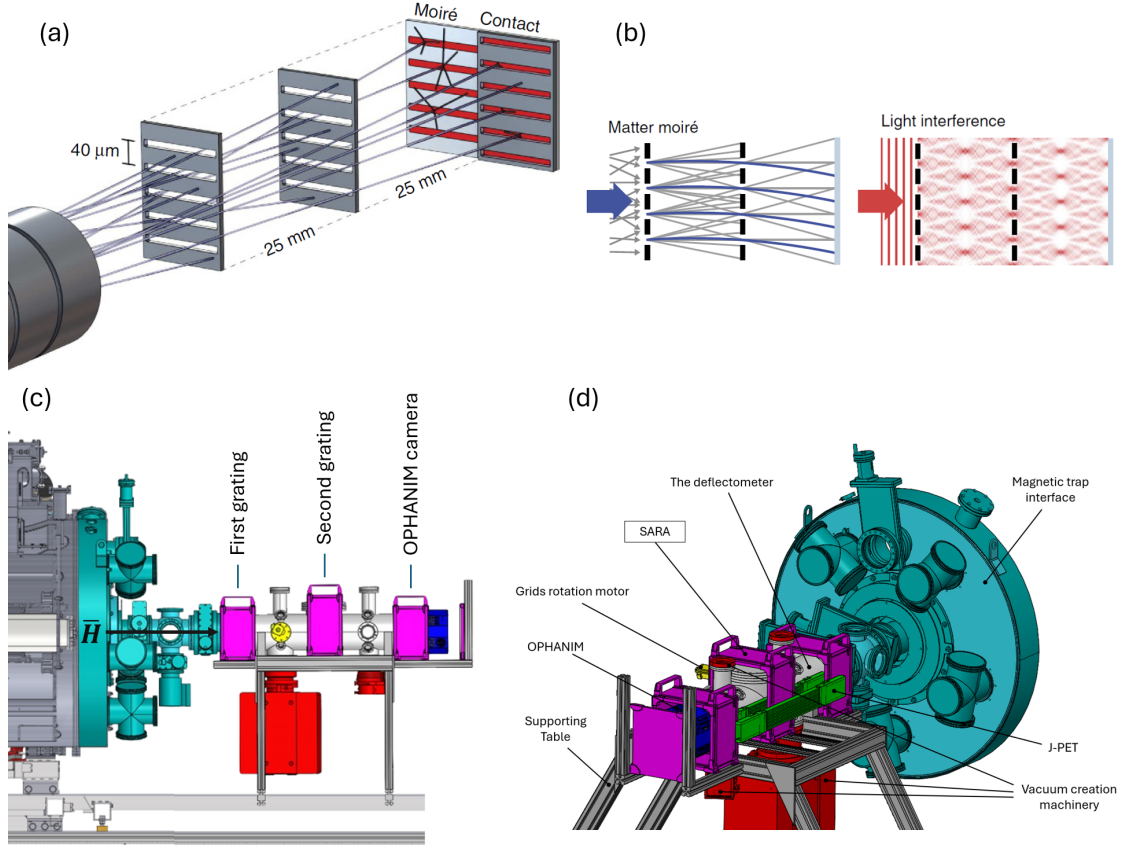


**Figure 1:** (a) (b) The deflectometer functioning principle [8], (c) (d) The Gravity Module

In this paper is presented and discussed the work performed to design and commission SARA (Scintillator Assemblies to Reveal Annihilations), the system of scintillators that aims to measure the time-of-flight distribution of antihydrogen atoms as they move through the moiré deflectometer. This information will be essential to the determination of the antimatter gravity acceleration and its collection will be achieved by detecting the annihilation products generated by the interaction between the antiatoms, the two gratings and OPHANIM.

## 2 Objective Statement, Requirements, Design and Commissioning

### 2.1 The Objective Statement

The main goal of the SARA detector is to measure the time-of-flight distribution of antihydrogen atoms by detecting their annihilation products (in particular pions) generated when they collide with either one of the two moiré gratings or the OPHANIM detector surface.

## 2.2 SARA Major Requirements

The scientific objective of SARA can only be achieved if it meets with the following requirements:

1. The detector shall have a temporal resolution in the order of the nanosecond to be able to properly map the time-of-flight distribution of antihydrogen. This ability grants the possibility to clearly discriminate different antihydrogen annihilations and discard the flash of pions and gamma rays produced when  $\bar{H}$  is formed.
2. The detector efficiency shall be as high as possible due to the rapidity of the antihydrogen transit event.
3. The detector shall clearly distinguish the annihilations that happened at the two gratings and at OPHANIM separately.
4. The detector shall allow the utilization of coincidence discrimination to remove the principal background noise sources (dark counts, cosmic noise, the CERN laboratory radioactive background noise) from the data to simplify their interpretation.

## 2.3 Initial Design Assumptions

Starting from the requirements just presented, it was decided to adopt the combination of plastic scintillators and Silicon Photomultipliers (SiPMs) as the technology to reveal annihilations. The former have been chosen both for their fast rise time (often lower than 1 ns) and the high detection efficiency. It was also concluded that a thickness of around 1 cm would generate a sufficient amount of photons during the transit of the annihilation generated pions. The material selected is the general purpose BC-404 from Luxium Solutions, of which some 1 m long, 13 mm thick panels were already available and whose properties are collected in Table 1. On the other hand, the SiPMs were selected after a trade off compared them with photomultiplier tubes (PMTs) as alternative. Even if PMTs offer superior performance in terms of dark count rates at room temperature, SiPMs are notoriously much less affected by the presence of stray magnetic fields, which means that, contrarily to PMTs, they do not require complex shielding, keeping the detector footprint compact; in addition, PMTs usually require bulky light guides.

**Table 1:** The BC-404 properties [9], [10]

Property	Value
Name:	Luxium Solutions BC-404
Base:	Polyvinyl-toluene
Panels dimensions (mm):	1000x277x13.3
Refractive index:	1.58
Rise time (ns):	0.7
Decay time (ns):	1.8
Wavelength of max. emission (nm):	408
Light attenuation length (cm):	140
Light output (n. photons/MeV):	10800



In order to maximize the detection efficiency and to efficiently remove the atmospheric muons background noise, while keeping the design as simple as possible, it was decided to assemble twelve rectangular plastic scintillators in three boxes to be placed around the gratings and the OPHANIM's detecting surface, partially covering the solid angle around them, and add one more rectangular scintillator panel behind the final detector; the result can be appreciated in Figure 3 (a). Given the limited space around the deflectometer, the on-axis dimension of the scintillator panels was fixed to 200 mm. Moreover, the necessity of performing baking procedures to obtain the ultra high vacuum inside the tube, coupled with the high sensitivity of BC-404 to high temperatures, imposed the definition of a box architecture that allows fast SARA integration and removal procedures. A test was performed to understand whether the application of mica insulation layers between the deflectometer and the scintillators could have prevented material damages and it was found that it is impossible to leave SARA intact during the baking. The boxes architecture selected is made of an upper part, containing the two vertical and the upper horizontal scintillators, and a lower part, containing the remaining panel (Figure 3 (b)). In order to integrate SARA's boxes on the instrument, first the lower part has to be placed in its correct position, then the upper part has to be lowered from above and finally, by applying four screws at the four bottom corners of the created box, the two parts are fastened both together and to the instrument supporting structure.

The last dimension of the boxes panels (the thickness was fixed to 13.3 mm and the width to 200 mm) was determined according to the SARA's surrounding and the thirteenth panel's dimensions were derived from the starting BC-404 material panels plus the decision of having this scintillator centered on the deflectometer axis. In particular, all the horizontal scintillators of the boxes are 316 mm long, the central box has vertical scintillators 316 mm high and the first and third boxes have vertical scintillator panels 270 mm high. Concerning the final scintillator, it is 275 mm wide and 318 mm high. It was performed an estimation of the percentage of the solid angles around each annihilation point that SARA is able to cover. The calculation has been made with a simple Monte Carlo simulation considering  $10^6$  randomly generated directions per annihilation point. The results are reported in Figure 2 and Table 2.

**Table 2:** Percentage of the solid angles around the annihilation points that are covered by SARA

Annihilation point	SARA parts considered	Percentage calculated
First grating	First box	66.2
Second grating	Second box	64.1
OPHANIM	Third box and final panel	71.1

The whole deflectometer apparatus, included SARA, will lay on a single supporting table made of Bosch profiles with various section dimensions. In particular, each box of scintillators, after the integration in the moiré structure, will be supported by two horizontal and parallel beams with section variable between the 20x20 mm, 30x30 mm and 45x45 mm sizes, while the final panel will be supported by one or two horizontal beams plus two vertical beams for stability; their section will vary as well due to the fact that the table will be built by assembling as much already available profiles as possible. This implied that SARA had to be designed granting adaptability to various section dimensions and to beams orientation parallel or orthogonal to the deflectometer axis.

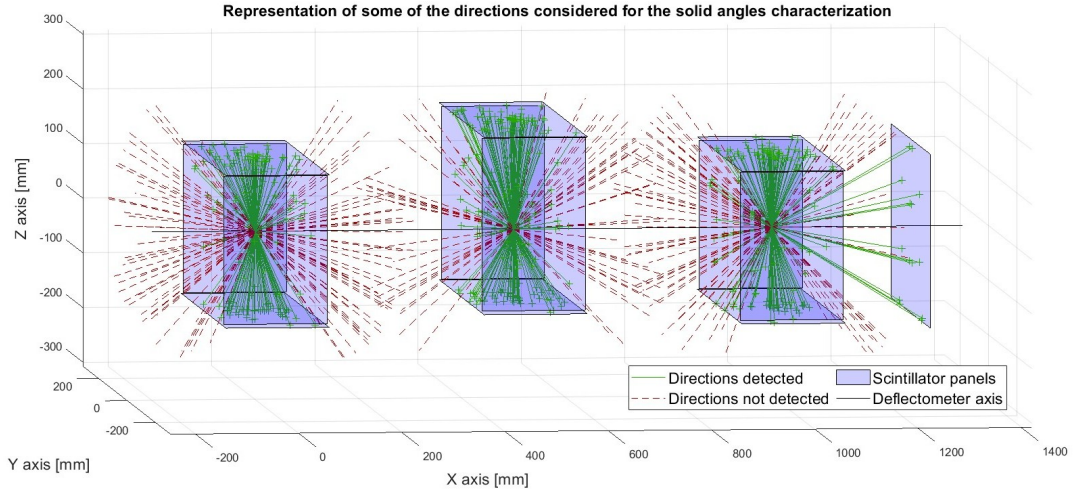


**Figure 2:** Some of the directions considered to determine the SARA covering percentage

## 2.4 The SARA's Structure

Given the thickness of the scintillator panels, they have been exploited as structural elements for the boxes, that have been designed to be obtained by connecting the panels by means of custom 3D printed corner elements, by some aluminum bars and two handles. The material selected to 3D print the corner elements is Nylon PA12 [11], chosen for its good mechanical properties over economic cost ratio, and the printing technology selected was the Multi Jet Fusion, that grants good isotropy of the final products. A trade-off analysis was conducted to compare a plastic 3D printed corner elements solution with a design obtained by welding metal plates. Despite more economic, the latter solution was discarded because of the unavoidable imprecision imposed by the welder's ability and the long-term damages at the points of contact between the scintillators and the metal panels edges; moreover the first alternative had also the advantage of minimizing the overall SARA's weight, important for its supporting structure architecture.

The shape of the corner elements was determined according to their structural function, their role in protecting the scintillators corners from accidental impacts, the minimization of their mass and the simplicity of the 3D printing process. In addition, the design process focused on the realization of as much equal components as possible, feature that allowed to reduce their unitary cost thanks to the policy of the manufacturer. The result is shown in Figure 3 (d).

Moving to the aluminum bars and handles, which hold the corner elements in place and facilitate handling, they have both been selected among COTS products. For the former aluminum 6060 T5, 15x3 mm section, 2 m long bars have been considered and for the latter the Elessa M.443/200-CH-C9 handles were chosen. To connect corner elements, aluminum bars and handles, the firsts hve been equipped with ensats, brass cylindrical inserts with a thread on the inside and designed to be hot-inserted in dedicated holes inside plastic components; the only disadvantage of this solution is to impose a minimum depth and walls thickness for the insertion holes, which slightly conflicts with the minimization of the printed material. In Figure 3 (e), the two selected products from Ruthex are shown.

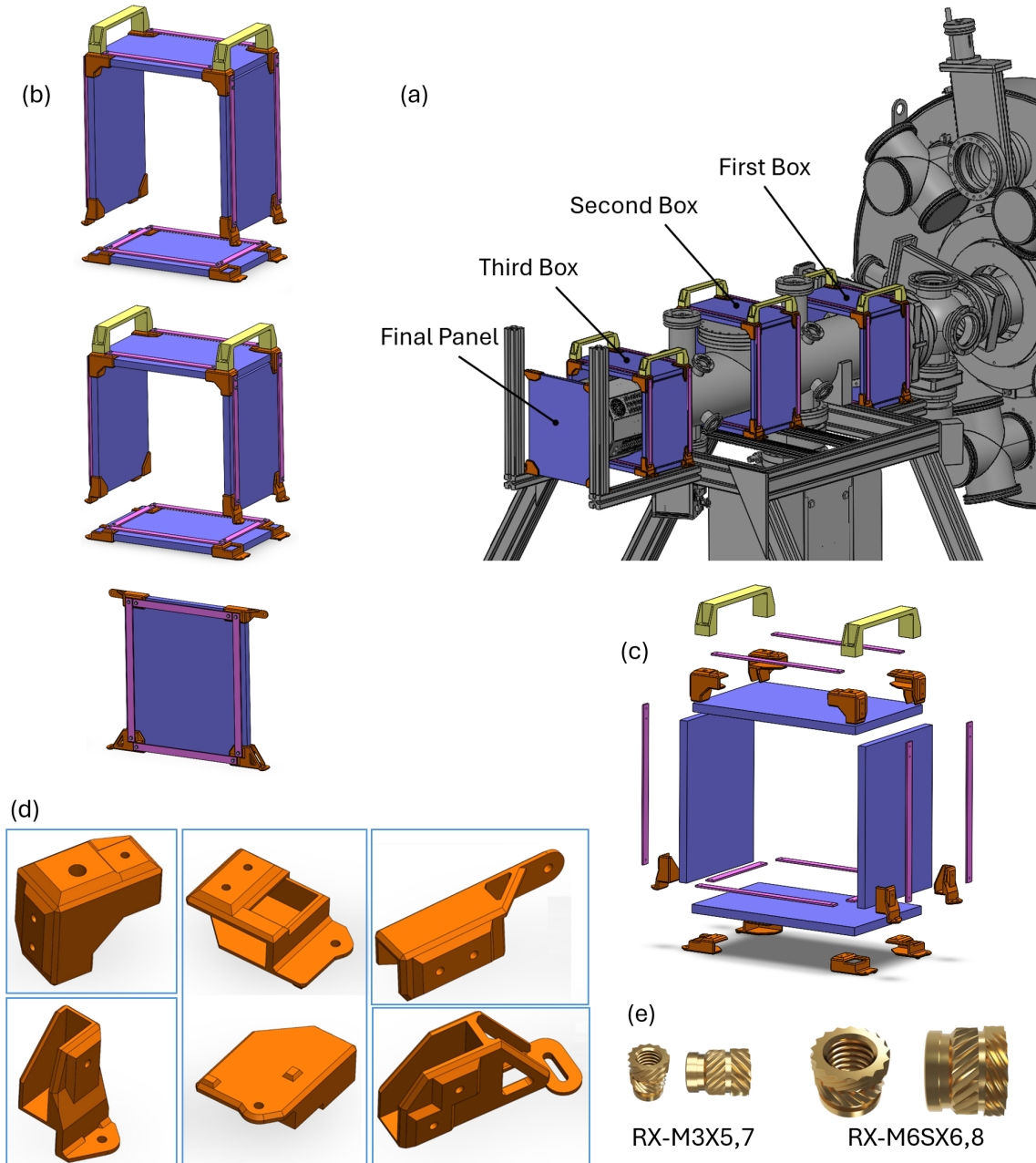


**Figure 3:** (a) SARA integrated in the AEgIS apparatus, (b) The SARA's main parts, (c) Exploded view of the first SARA's box, (d) The variants of corner elements (e) The ensats selected

## 2.5 The FEM Mechanical Simulations

Beside all the physical tests performed, it was decided to support the whole design process with mechanical finite elements analysis, using Autodesk Fusion as simulating software. In particular, the focus was directed to the central box, which is the bulkiest and so the one representing the critical case for the mechanical stress. The analysis mainly investigated four loading conditions and it also simulated both the nominal and the overloaded scenarios described in Table 3. In the first loading condition, already fastened to the instrument supporting structure, the box is loaded with a horizontal force applied on one of its upper edges; this load condition can also occur when only the upper part is fastened to the box supports and simulates an accidental impact with the box after it has been integrated into the instrument. In the second and third cases, a horizontal load is applied respectively inward and outward at a lower edge of the upper part; these two load combinations simulate an accidental impact that can happen during the upper part integration or removal. Finally, in the fourth load condition the central box is supported by 20x20 mm Bosch profiles that run parallel to the deflectometer axis. In this case, where the gap between the supporting beams is larger than the lower horizontal scintillator length, the whole weight of the box is managed by the corner elements alone. Given the high deformation at break of Nylon PA12, maximum displacement was used as an indicator of stiffness. The results of the analysis are reported in Figure 4 and Table 4.

**Table 3:** The two scenarios considered in the FEM analysis

Quantity	Nominal scenario	Overloaded scenario
Force (N)	10.0	15.0
Gravity acceleration (g)	1.00	1.35

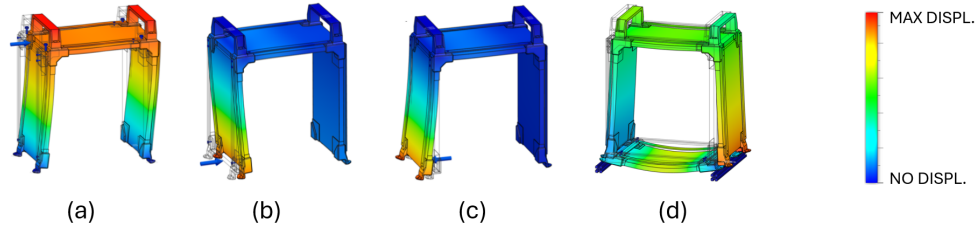


**Figure 4:** The FEM analysis computed deformations. The blue arrow represents the applied force and gravity is directed downward. (The displacement is exaggerated for illustration purposes)

**Table 4:** The maximum displacements computed with the FEM analysis

Case	Nominal Scenario (mm)	Overloaded Scenario (mm)
(a)	0.443	0.670
(b)	0.997	1.497
(c)	1.659	2.497
(d)	0.122	0.133

## 2.6 The Readout Electronics

Concerning the electronics design, it was decided to apply on every scintillator panel one PCB hosting twelve SiPMs, to be divided into two groups of six, each one equipped with a dedicated output port, with the possibility to read them either in coincidence or in parallel. It was initially decided to mount each PCB on one lateral side of the rectangular scintillators, using nylon screws as fastening strategy due to their reversibility, effectiveness and low cost. For this reason, the PCBs have been designed to be elongated, as wide as the thickness of the scintillators and equipped with four screw holes. In order to support this design choice a preliminary test was performed, analyzing the average output amplitude of a PCB hosting 3 SiPMs first mounted on a lateral side of a SARA scintillator and then on one of its two main surfaces, as represented in Figure 5 (a). The high-energy particles source used was atmospheric muons and the result of the two acquisitions was practically identical. Consequently, the lateral mounting position was selected for the better cable management granted and basing on the reasonable assumption that a SiPM on a lateral surface has a direct view on a wider volume of the scintillator compared to one on a main surface. Moving to the verification of the design hypothesis to fasten the PCBs with nylon screws, a test was carried out to determine how to create threaded holes in the scintillator panels, if feasible; the result of the test is shown in Figure 5 (b). It was found that it is possible to create the desired threaded holes, but the procedure developed is time-consuming and complex, moreover any error could damage the entire scintillator panel due to its extreme sensitivity to heat; for this reasons it was concluded to move to black tape as a still reversible and economical solution to secure the PCBs.

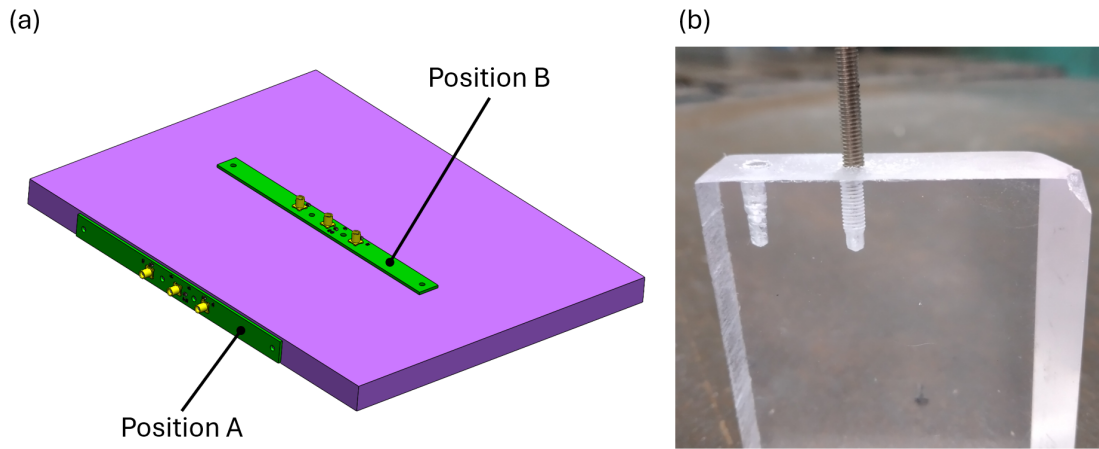


**Figure 5:** (a) The two PCB positions tested, (b) The result of the threaded hole creation test

The model of SiPM selected is the Hamamatsu S14160-3050HS [13]. The choice was mainly driven by its peak sensitive wavelength, which closely matches the maximum emission wavelength of BC-404, and its compact dimensions (3.4x3.4x1.35 mm), tailored for the lateral side application. Some of the chosen SiPM's properties are collected in Table 5.

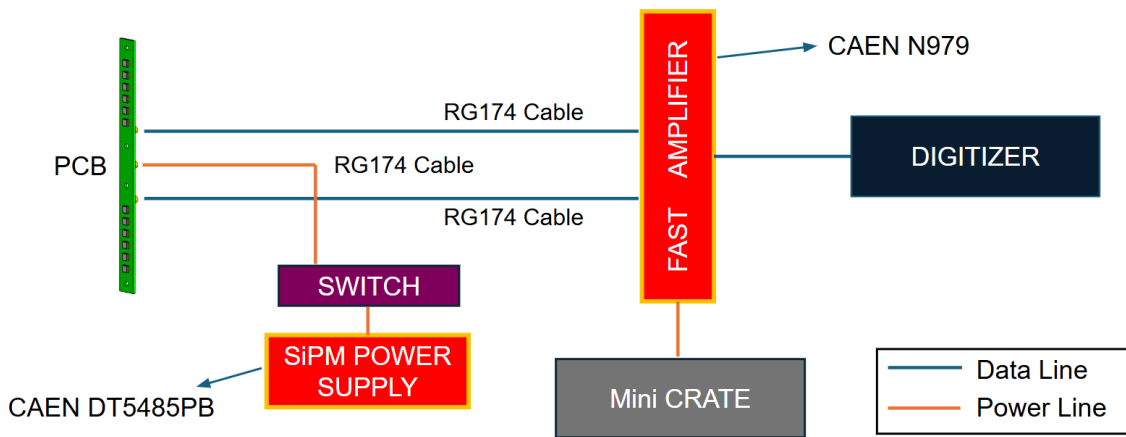
The PCBs architecture developed, shown in Figure 7 (a), is based on the realization of two independent channels where six SiPMs are powered in parallel by a unique powering line that operates at 4 V above the breakdown voltage. Their outputs are also connected to a single output line, that is then read exploiting the discharge of a capacitor with capacitance 100 nF (C11 and C21

**Table 5:** Characteristics of the Hamamatsu S14160-3050HS

	Quantity	Value	Unit of measure
Effective photosensitive area		3.0x3.0	mm <sup>2</sup>
Window refractive index		1.57	- -
Spectral response range		270 to 900	nm
Peak sensitive wavelength		450	nm
Recommended operational voltage		38 + 2.7	V
Dark current (nominal - maximum)		0.6 - 1.8	μA
Gain		2.5 x 10 <sup>6</sup>	- -
Terminal capacitance		500	pF

in the figure), measured as the voltage variation at the two ends of a 1 kΩ resistance connected in series (R11 and R21). The goal for the PCB architecture design was to obtain a straightforward solution. In order to enable the 12 SiPMs in-parallel reading strategy, a short-circuit bridge can be applied to a central 3 pins connector, moreover, due to the particular shape selected for the PCBs, the SiPMs have been aligned to form two six elements strips in the direction of the PCB main dimension. To improve the interaction between the detectors and the plastic scintillators, it was decided to apply an optical grease at the contact surface, after a comparison test confirmed an increase in the number of detected muons scintillations.

Moving to the overall electronics setup, it was decided to power all the PCBs with a single SiPMs power supply, the CAEN DT5485PB, exploiting a single input-13 outputs custom made switch. It was also decided that all the PCBs outputs have to be collected by a G=10 fast amplifier, the CAEN N979, that subsequently sends the amplified signals to a 14-bit digitizer for the data acquisition. Both the power and data lines use coaxial cables (RG174) with LEMO connectors. A representation of the SARA's electronics architecture is reported in Figure 6.

**Figure 6:** The SARA's electronics architecture



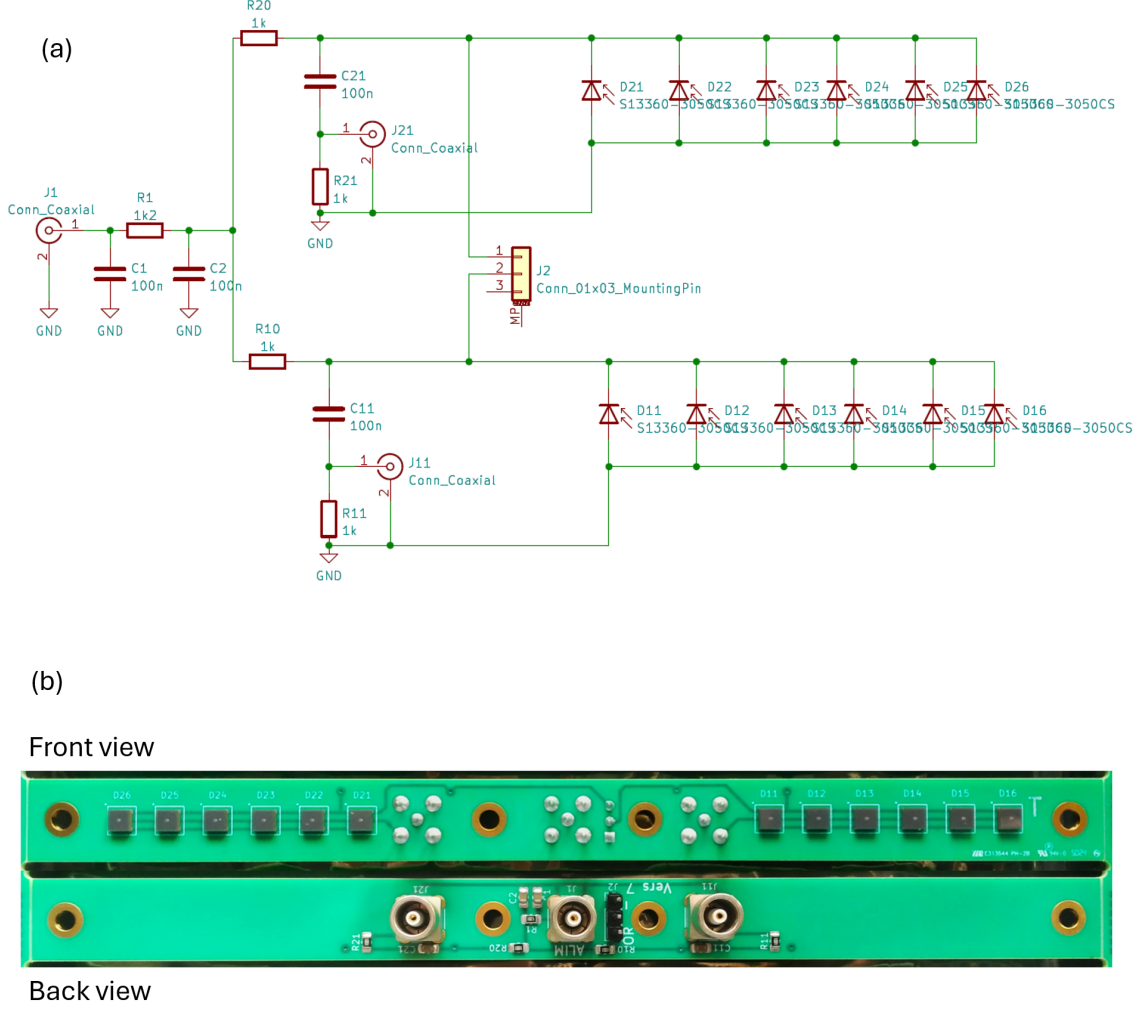


**Figure 7:** (a) The PCB scheme (b) Front and back views of a manufactured SARA's PCB

## 2.7 The SARA performance optimization

Regarding the performance of the SARA scintillators, two goals were considered: to maximize the amount of light reaching the SiPMs and to prevent external light infiltrations. To achieve the first goal, it was concluded that all the six faces of the rectangular scintillator panels had to be polished and they also had to be wrapped with aluminum foil with the reflective side facing inward; the aluminum reflective surface had to be cleaned and flattened before the application. To achieve the second feature, it was determined that, after the integration of aluminum foil and detectors PCB, the scintillators had to be covered with an obscuring material. Specifically, the one selected was OPAQ-1152i from Luminis Films, a black PVC foil designed to block visible light. Its selection was justified by the results of the test performed to measure its absorbance and to compare it with the typical emission spectrum of LED and fluorescent lamps. The absorbance was calculated as:

$$A(f) = \log_{10} \frac{\Phi_R(f)}{\Phi_S(f)} \quad (2.1)$$



where  $\Phi_R(f)$  is the intensity as function of the frequency of a reference light ray and  $\Phi_S(f)$  is the intensity of an identical light ray after it pierced the tested material. By analyzing the results of the test, shown in Figure 8, it is possible to appreciate a Gaussian behavior of the absorbance when moving toward lower wavelengths, before the spectrophotometer used for the test, a PerkinElmer Lambda 650, reaches saturation and starts to give unreliable values. Based these results, it was concluded that the chosen light protection material has an absorbance greater than 6 in the region of the visible spectrum where LED and fluorescent lamps emit most of their power.

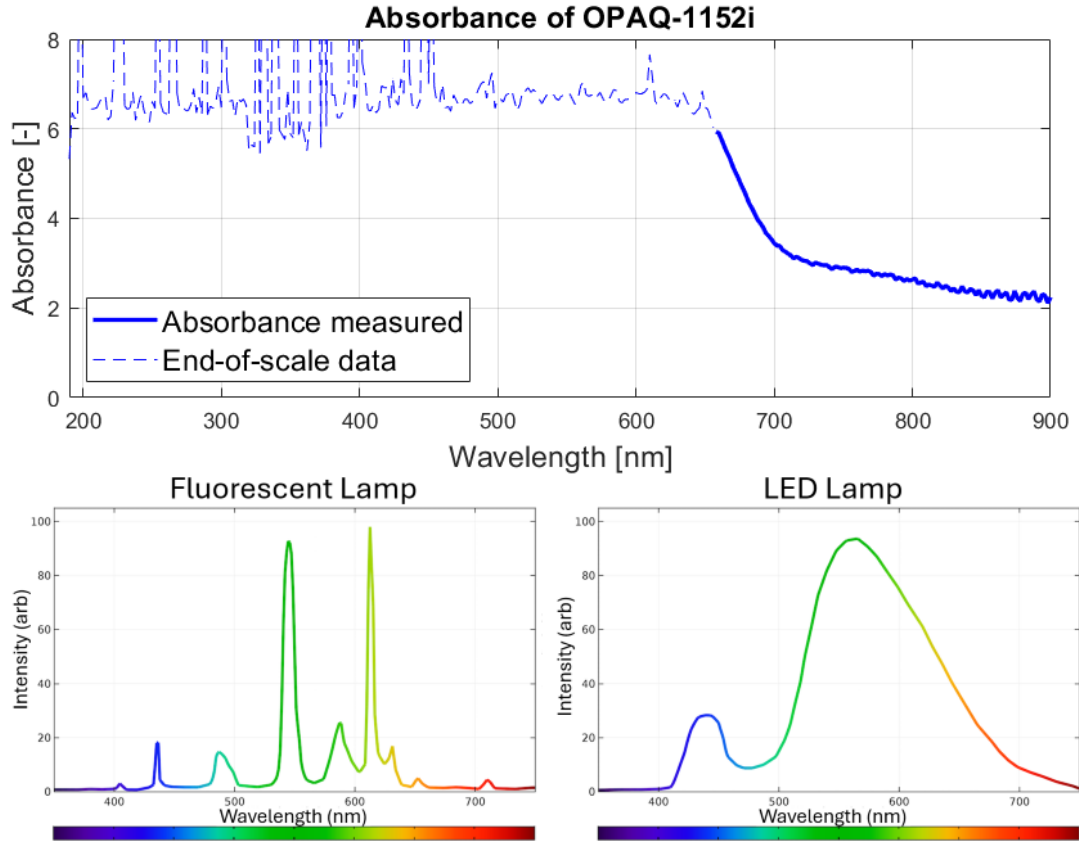


**Figure 8:** OPAQ-1152i absorbance and emission spectrum of LED and Fluorescent lamps [12]

## 2.8 The SARA Commissioning

After the conclusion of the design phase, the construction process started, yielding the results shown in the following figures. In Figures 9 - 1. and 2. are represented some scintillators after being polished and some others wrapped in the aluminum foil; the appreciable rectangular holes allow the SiPMs to have an optical contact with the scintillator. In Figures 9 - 3. and 4. are shown a scintillator with its detectors PCB secured using black tape and three completed SARA's scintillators, now also wrapped in OPAQ-1152i. Figures 9 - 5. and 6. show some corner elements with ensats already hot-inserted and the first completed SARA's box (which was the central one). Finally, Figure 10 shows the whole instrument before the completion of the detectors integration

and Figure 11 shows the average output collected from the two channels of a SARA's scintillator operated in parallel mode and tested with muons.



**Figure 9:** Construction process of the SARA scintillation detector. 1. Some of the polished scintillator panels, 2. Some scintillators wrapped in aluminum, 3. A PCB applied on a scintillator, 4. Three scintillators wrapped in OPAQ-1152i, 5. Some corner elements after the hot insertion of the inserts, 6. The first completed SARA's box



**Figure 10:** The complete instrument before the completion of the integration of the PCBs

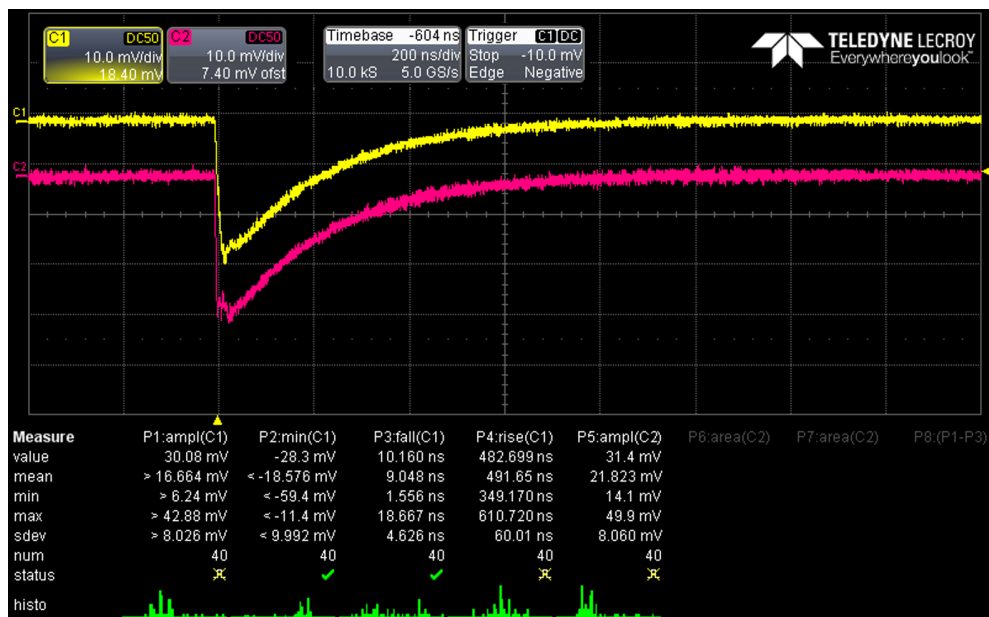


**Figure 11:** The average output obtained from the two channels of a SARA scintillator when operated in parallel mode

Concerning the efficiency of the scintillators, the procedure of calculation exploited the fact that the scintillators composing the boxes come in just two sizes, with eight elements in the first pool (316 mm long panels) and four elements in the second (270 mm long panels). By stacking three scintillators from the same group and using the double coincidence between the top and bottom ones as proof that a muon crossed the whole stack, the efficiency of the middle panel can be evaluated as the ratio between the number of triple coincidence (all three scintillators triggered) and



the one of double coincidences (only the reference panels triggered). This procedure was performed testing each scintillator of the two pools and the efficiency of the final panel (that comes in a unique piece) was estimated as the average value of all the other efficiencies. The coincidence counting has been achieved assembling three identical readout channels, each one composed by a delay line amplifier (ORTEC 460), and a single-channel discriminator (ORTEC 551). The amplifier received the signals from a scintillator and its unipolar output was sent to the discriminator, whose lower threshold was tuned to accept only the events characterized by the highest energies in order to cut most of the noise. The two identical outputs of each discriminator were then sent to two ORTEC 414A Fast Coincidence units, one receiving input from all three scintillators and the other from only the two reference panels; in this way the two counts were referred to the same events improving the reliability of the comparison. The efficiency measurement setup is represented in Figure 12 and the results of the analysis are collected in Table 6.

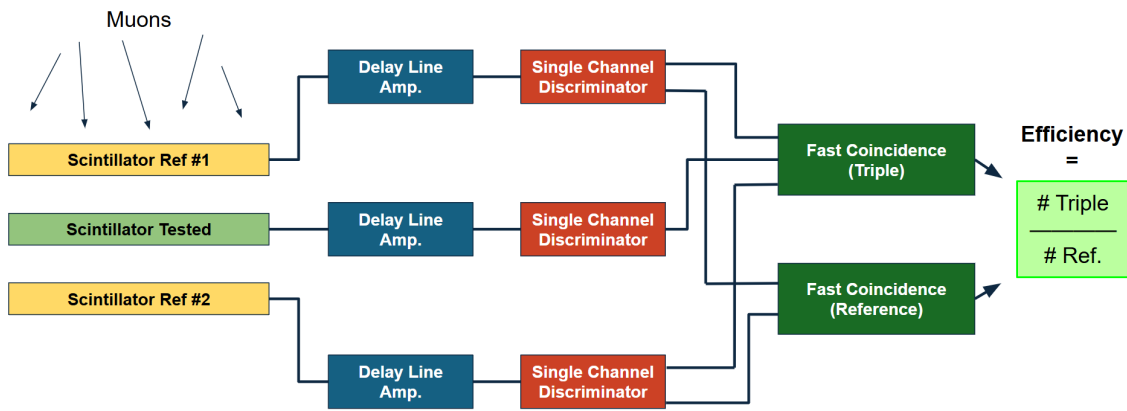


**Figure 12:** The efficiency measurement setup

**Table 6:** The scintillators efficiency

Scintillator	Efficiency measured	Scintillator	Efficiency measured
1	$0.84 \pm 0.04$	7	$0.84 \pm 0.04$
2	$0.87 \pm 0.04$	8	$0.76 \pm 0.04$
3	$0.79 \pm 0.04$	9	$0.77 \pm 0.04$
4	$0.86 \pm 0.04$	10	$0.84 \pm 0.04$
5	$0.82 \pm 0.04$	11	$0.79 \pm 0.04$
6	$0.89 \pm 0.04$	12	$0.81 \pm 0.04$
		13	0.82 (estimated)

It was also performed a measurement of the dark current of one of the PCBs, connected to the same power supply of the others, but not applied to any scintillator. The PCB was placed into a small box wrapped in multiple layers of obscuring material to prevent any possible influence of stray light. The result of the measurement, equal to  $1.15 \mu\text{A}$ , is in agreement with the datasheet supplied by Hamamatsu.

### 3 Discussion

According to all the physical tests performed, the numerical simulations and the output signals recorded during the first acquisition, it can be concluded that SARA clearly detects muons, which deposit in the scintillators an energy comparable to that of pions resulting from the annihilation between the antihydrogen and the deflectometer. From a mechanical perspective, it has been demonstrated, first with the tests performed to validate the design and later with the inspection of the final product, that SARA is structurally stiff and able to stand all the loads it will encounter during its operational life. The two-parts box architecture confirmed its effectiveness, indeed assembly and disassembly of the boxes is straightforward and rapid and the alignment between the various corner elements at the two parts conjunctions is nearly perfect in all three boxes. The decision of standardize the corner elements allows the boxes components to be symmetric, giving the possibility to rotate by  $180^\circ$  the upper and lower parts choosing in which direction the PCB output ports are oriented (along the deflectometer axis). No tests for the integration on the supporting table have been performed, since the latter has not been assembled yet, but, using spare Bosch profiles, it was performed a preliminary verification that validated the corner element design in terms of optimization of the scintillators system integration. Regarding the electronics, it should be noted that the current design does not fully exploit the fast response capabilities of the selected SiPMs. Additionally, due to the developed circuit architecture, in which all six SiPMs in a line are connected in parallel, their outputs do not sum as expected. This limitation was attributed to two possible reasons: the first is that the activation of a single SiPM during a scintillation event induces a small voltage variation across the shared 100 nF capacitor, leading to different gain responses among the SiPMs, and the second is the fact that connecting multiple SiPMs in parallel results in a higher overall capacitance, which affects the system signal characteristics. Nevertheless, it was verified that the high number of SiPMs considered still increases the number of scintillation events detected (by comparing it with the 3 SiPMs PCB used for the initial tests, which has an identical circuit concept and was operated using same powering voltage and trigger on the output voltage variation). It is also important to note that the signal measured during the first acquisition campaign using muons as energetic particles (the one shown in Figure 11) has an excellent signal-to-noise ratio, even without being amplified by the CAEN N979. In addition, the efficiency characterization given satisfactory results, with an average of 0.82 and limited variation among different scintillators. This enforces the conclusion that SARA will be able to detect the majority of the annihilation products generated at the two gratings and OPHANIM.

Taking stock of everything that has been presented, it can be concluded that SARA will be able to accomplish its objective contributing to the measurement of the effects of gravity on antimatter.

### 4 Acknowledgments

The use of the scintillators from the concluded ATRAP collaboration is gratefully acknowledged. Special thanks are extended to Veronica Marzo for her contribution to the efficiency measurement. The project was funded by Politecnico di Milano.

*In memory of Sara Conte*

## References

- [1] A. Kellerbauer et al. (AEgIS Collaboration), *Proposed antimatter gravity measurement with an antihydrogen beam*, *Nucl. Instrum. Meth. B* **266** (2008), [[arXiv:2306.04594](#)].
- [2] M. Charlton, S. Eriksson, G. M. Shore, *Antihydrogen and Fundamental Physics, First Edition*, Springer Cham, (2020).
- [3] Z. Zhang, *The detection of cold antihydrogen atoms*, PhD Thesis, Bochum University (Germany), Fakultät fuer Physik und Astronomie, (2007).
- [4] M. Berghold et al. (AEgIS Collaboration), *Real-time antiproton annihilation vertexing with submicrometer resolution*, *AAAS* **11** (2025), [[arXiv:2406.16044](#)].
- [5] C. Amsler, M. Antonello, A. Belov et al., *Pulsed production of antihydrogen*, *Commun. Phys.* **4** (2021).
- [6] S. Mariazzi et al. (AEgIS Collaboration), *High-yield thermalized positronium at room temperature emitted by morphologically tuned nanochanneled silicon targets*, *J. Phys. B: At. Mol. Opt. Phys.* **54** 085004 (2021) .
- [7] M. Charlton, *Antihydrogen production in collisions of antiprotons with excited states of positronium*, *Physics Letters A* **143** (1990).
- [8] S. Aghion, O. Ahlén, C. Amsler et al., *A moiré deflectometer for antimatter*, *Nat Commun* **5**, 4538 (2014).
- [9] [Luxium Solutions: BC-400, BC-404, BC-408, BC-412, BC-416](#).
- [10] E. Quintos, C. Fernández, L. Rebolledo-Herrera, E. Moreno, *Intrinsic time resolution and efficiency study for simulated scintillators plastics with Geant4*, *Revista Mexicana de Física* **69** (2023).
- [11] [Weerg: Nylon PA12 Properties](#).
- [12] D. Smith, *Calculating the emission spectra from common light sources*, *COMSOL Blog* (2016).
- [13] [Hamamatsu: S14160-3050HS](#).